

# Crack Path Simulation by the MVCCI Method and Experimental Verification for Curved Fatigue Cracks in the Neighbourhood of a Circular Hole

H. Theilig, M. Wünsche and R. Bergmann

Department of Mechanical Engineering, University of Applied Sciences Zittau/Görlitz,  
Postfach 1455, D-02754 Zittau, Germany, e-mail: h.theilig@hs-zigr.de

**ABSTRACT.** *The Modified Virtual Crack Closure Integral (MVCCI) method has been proved to be a highly effective numerical procedure for the analysis of various crack problems in linear elasticity. In the present paper it will be shown that the MVCCI method in conjunction with multiple mesh analysis can also readily be utilised for the numerical prediction of curved fatigue crack growth under proportional loading conditions. Further it will be shown that the common computer-aided two-dimensional crack path prediction can be considerably improved in accuracy by using a predictor-corrector procedure. In combination with the MVCCI method, this results in a step-by-step parabolic approximation of the simulated crack path. By this method both the new locus of the crack tip and the slope of the crack path at this point can be computed simultaneously by the SIFs by only one virtual tangential crack extension with respect to the previous step.*

*In order to evaluate the validity and efficiency of the proposed higher order crack path simulation method in relation to the well-established basic strategies, experiments of curved fatigue crack growth in the neighbourhood of a circular hole are carried out with two specially designed specimens under proportional lateral force bending. In all cases considered, the computationally predicted crack trajectories show an excellent agreement with the different types of curved cracks that are obtained in the experiments as a function of the position of crack initiation.*

## INTRODUCTION

The failure of structures and components is often caused by cracks that frequently originate and extend in regions characterised by complicated geometrical shapes and asymmetrical loading conditions. In such cases, the developing crack paths are found to be curved. Several simulation methods have been proposed for crack path predictions based on step-by-step analyses using finite elements or boundary elements (Bergquist and Gnex [1], Sumi [2,3], Portela and Aliabadi [4]). In the present paper, attention is focused on a new predictor-corrector method (PCM) that results in an incremental parabolic approximation of the crack path on the basis of quantities which the straightforward Modified Virtual Crack Closure Integral Method can provide (Theilig, Döring and Buchholz [5-8]). In order to show the significance of the proposed technique, computational results are

compared with findings from experimental investigations obtained by the aid of a specially designed specimen with a circular hole under lateral force bending.

## TWO-DIMENSIONAL CRACK PATH PREDICTION

Consider a crack in a two-dimensional linear elastic body under proportional mixed-mode loading conditions. The stresses ahead of the crack tip are given by

$$\begin{aligned}\sigma_{11}(x_1, 0) &= \frac{k_I}{\sqrt{2\pi x_1}} + T + b_I \sqrt{\frac{x_1}{2\pi}} + O(x_1), \\ \sigma_{22}(x_1, 0) &= \frac{k_I}{\sqrt{2\pi x_1}} + b_I \sqrt{\frac{x_1}{2\pi}} + O(x_1), \\ \sigma_{12}(x_1, 0) &= \frac{k_{II}}{\sqrt{2\pi x_1}} + b_{II} \sqrt{\frac{x_1}{2\pi}} + O(x_1),\end{aligned}\tag{1}$$

where  $k_I$  and  $k_{II}$  are the stress intensity factors (SIFs).  $T$ ,  $b_I$  and  $b_{II}$  are the included higher order stress field parameters. It is known that in such a situation the crack will propagate in a smoothly curved manner after an abrupt deflection out of its original plane, Fig. 1.

The generalisation of the local symmetry criterion can be regarded as the basis for the evolution of the crack path. Therefore the state of stress ahead of the deflected new crack tip exhibits no  $K_{II}$  and is given by

$$\begin{aligned}\sigma_{11}(x_1^*, 0) &= \frac{K_I}{\sqrt{2\pi x_1^*}} + T^* + b_I^* \sqrt{\frac{x_1^*}{2\pi}} + O(x_1^*), \\ \sigma_{22}(x_1^*, 0) &= \frac{K_I}{\sqrt{2\pi x_1^*}} + b_I^* \sqrt{\frac{x_1^*}{2\pi}} + O(x_1^*), \\ \sigma_{12}(x_1^*, 0) &= b_{II}^* \sqrt{\frac{x_1^*}{2\pi}} + O(x_1^*).\end{aligned}\tag{2}$$

It can be stated that continuous crack deflections can be caused only by the existing non-singular stresses.

According to Sumi [2,3] the crack path prediction can be performed by using the first order perturbation solution of a slightly kinked and curved crack. A virtually extended slightly kinked and smoothly curved crack path profile (Fig. 2) is assumed in the form

$$l(x_1) = \alpha x_1 + \beta x_1^{3/2} + \gamma x_1^2 + O(x_1^{5/2}),\tag{3}$$

where  $\alpha$ ,  $\beta$  and  $\gamma$  are the shape parameters.

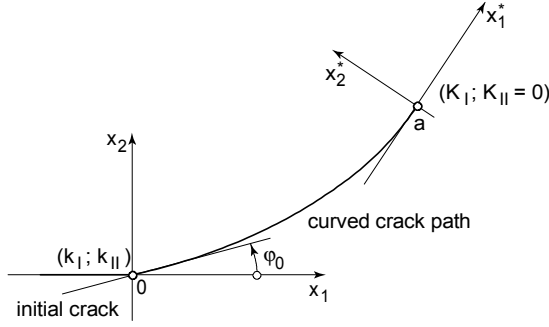


Figure 1. A kinked and curved crack.

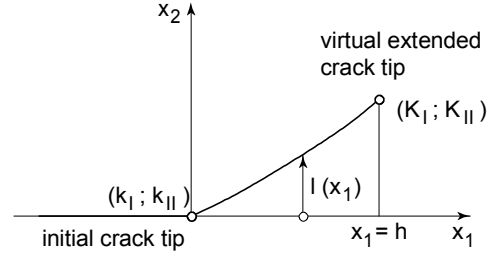


Figure 2. Virtually extended crack.

As a consequence of the crack propagation criterion of local symmetry the SIF  $K_{II}$  vanishes along the smooth crack path and the shape parameters of the natural crack geometry are obtained as

$$\alpha = -2k_{II}/k_I, \quad \beta = \frac{8}{3}\sqrt{\frac{2}{\pi}}\frac{T}{k_I}\alpha, \quad (4)$$

$$\gamma = -\left(k_{II}\bar{k}_{22} + k_I\bar{k}_{21} + \frac{b_{II}}{2}\right)\frac{1}{k_I} + \left\{\left[k_I(2\bar{k}_{22} - \bar{k}_{11}) + \frac{b_I}{2}\right]\frac{1}{2k_I} + 4\left(\frac{T}{k_I}\right)^2\right\}\alpha$$

where the quantities  $\bar{k}_{11}, \bar{k}_{21}, \bar{k}_{22}$  represent the effects of the far field boundary conditions on the crack growth. If we consider a crack under local symmetry at the initial crack tip, i.e.  $k_{II} = 0$ , we find  $\alpha = \beta = 0$ . Therefore the parabolic crack profile

$$l(x_1) = \gamma x_1^2, \quad \gamma = -\left(\frac{b_{II}}{2} + k_I\bar{k}_{21}\right)\frac{1}{k_I} \quad (5)$$

holds. In this case, the crack will propagate without kinking with a continuous deflection. But in the case of a self-similar virtual crack extension of the postulated straight crack the SIFs

$$\bar{K}_I = k_I + \left(\frac{b_I}{2} + k_I\bar{k}_{11}\right)h, \quad \bar{K}_{II} = \left(\frac{b_{II}}{2} + k_I\bar{k}_{21}\right)h \quad (6)$$

are obtained. Finally for a selected increment  $\Delta h$  one obtains the following geometrical information of the real crack path

$$\Delta\varphi = -2\frac{\Delta\bar{K}_{II}}{k_I}, \quad \Delta l = -\frac{\Delta\bar{K}_{II}}{k_I}\Delta h, \quad \Delta a \approx \Delta h \left[1 + \frac{2}{3}\left(\frac{\Delta\bar{K}_{II}}{k_I}\right)^2 - \frac{2}{5}\left(\frac{\Delta\bar{K}_{II}}{k_I}\right)^4\right]. \quad (7)$$

It can be seen that under the local symmetry criterion  $K_{II} = 0$  the change of the slope

and the locus of the crack tip can be interpreted as the consequence of  $\Delta \bar{K}_{II} \neq 0$  for a virtual tangential crack extension  $\Delta h$  (Fig. 3). Therefore, in the case of proportional loading conditions the analysis of a smooth crack path can be carried out by a small virtual tangential crack extension as the predictor-step in combination with a finite change of the crack path as the corrector-step. On account of the predictor-step the calculation of  $K_I = \bar{K}_I$  and  $\Delta \bar{K}_{II}$  is necessary in conjunction with the related tangential crack extension  $\Delta h$ . From Eqs 7 the need for an efficient numerical mode separation technique in conjunction with the step-by-step analysis can be seen.

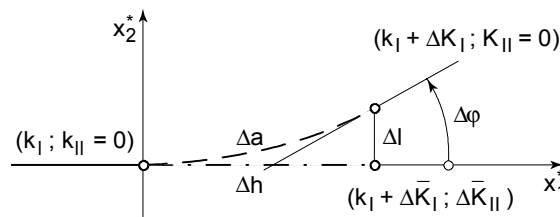


Figure 3. Step of a curved crack propagation.

## IMPROVED MVCCI METHOD

With respect to this requirement the MVCCI method has proved to be highly advantageous, because it delivers the separated strain energy release rates of the two modes simultaneously without any additional effort (Buchholz [8]).

For 8-noded quadrilaterals at the crack tip, which are necessary to model the parabolic

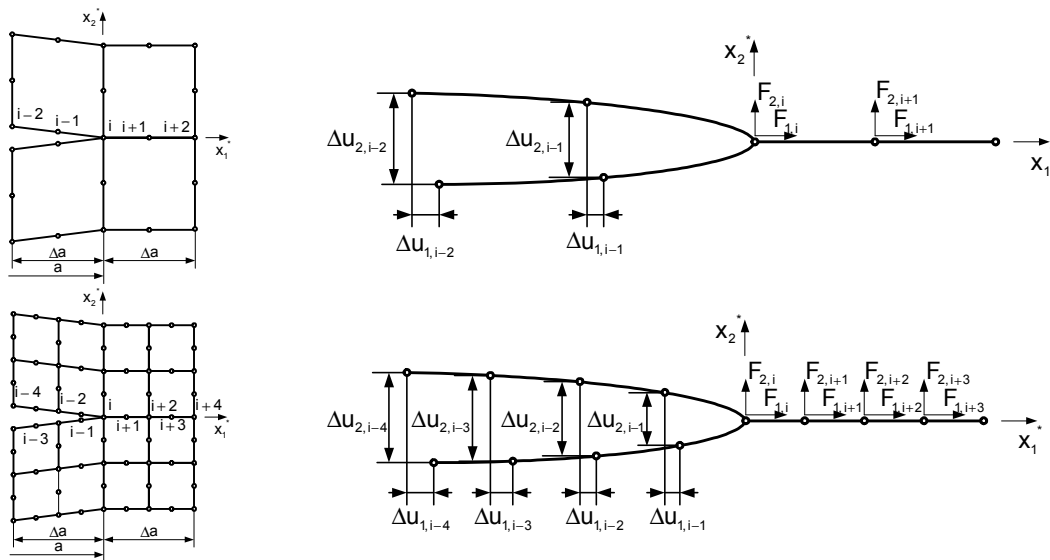


Figure 4. First and second order evaluation of the MVCCI method.

curved increments of the crack path, the following first and second order finite element representation of Irwin's crack closure integral relations can be given for the crack closure length  $\Delta a$ , Fig. 4:

$$\begin{aligned} G_I^{(1)}(a_i) &= \frac{1}{2t\Delta a} (F_{2,i}\Delta u_{2,i-2} + F_{2,i+1}\Delta u_{1,i-1}), & G_{II}^{(1)}(a_i) &= \frac{1}{2t\Delta a} (F_{1,i}\Delta u_{1,i-2} + F_{1,i+1}\Delta u_{1,i-1}), \\ G_I^{(2)}(a_i) &= \frac{1}{2t\Delta a} (F_{2,i}\Delta u_{2,i-4} + F_{2,i+1}\Delta u_{2,i-3} + F_{2,i+2}\Delta u_{2,i-2} + F_{2,i+3}\Delta u_{2,i-1}), & (8) \\ G_{II}^{(2)}(a_i) &= \frac{1}{2t\Delta a} (F_{1,i}\Delta u_{1,i-4} + F_{1,i+1}\Delta u_{1,i-3} + F_{1,i+2}\Delta u_{1,i-2} + F_{1,i+3}\Delta u_{1,i-1}). \end{aligned}$$

As the consequence of two calculations [9-11] with the same  $\Delta a$  and different element sizes  $h_1 > h_2$  in the neighbourhood of the crack tip the improved strain energy release rates are obtained as

$$G_I^{\text{IMPR}} = \frac{G_I^{(1)} - G_I^{(2)} \frac{h_1}{h_2}}{1 - \frac{h_1}{h_2}}, \quad G_{II}^{\text{IMPR}} = \frac{G_{II}^{(1)} - G_{II}^{(2)} \frac{h_1}{h_2}}{1 - \frac{h_1}{h_2}}. \quad (10)$$

The essential feature of this technique is, that SIFs of higher accuracy can be obtained by comparatively coarse mesh divisions.

## CURVED FATIGUE CRACK GROWTH TESTS

In order to evaluate the validity and the efficiency of the proposed higher-order crack path simulation method with respect to the well established basic strategies, experiments of non-coplanar fatigue crack growth were carried out with a specially designed specimen under cyclic lateral force bending (LFB). The LFBH specimen was designed with a hole in the centre in order to produce a non-homogeneous stress field (Fig. 5). Steel E335 was selected as specimen material.

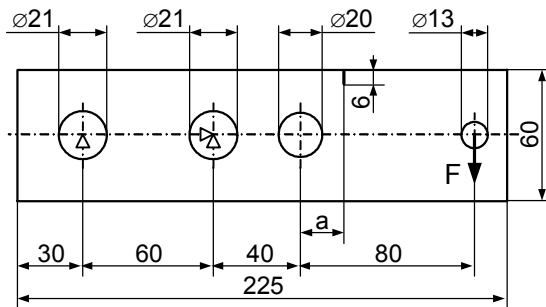


Figure 5. Dimensions and definition of the notch position  $a_N$  of the LFBH specimens (thickness  $t = 10$  mm).

Crack initiation from notches at different positions  $a_N$  along the tensile loaded edge of these specimens is investigated to produce different crack interactions with the hole. The notches have been manufactured with a width of 0.4 mm and a depth of 6 mm.

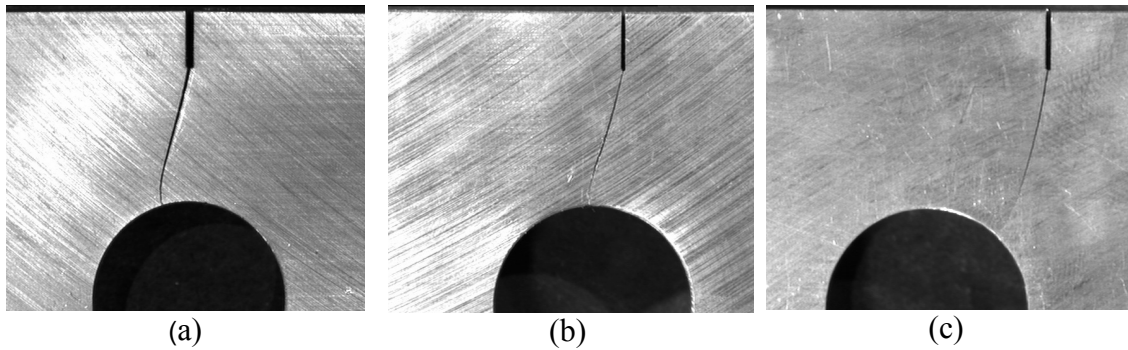


Figure 6. Experimental fatigue crack paths of specimens with different notch position  
 (a)  $a_N = 0$  mm; (b)  $a_N = 3$  mm; (c)  $a_N = 12$  mm.

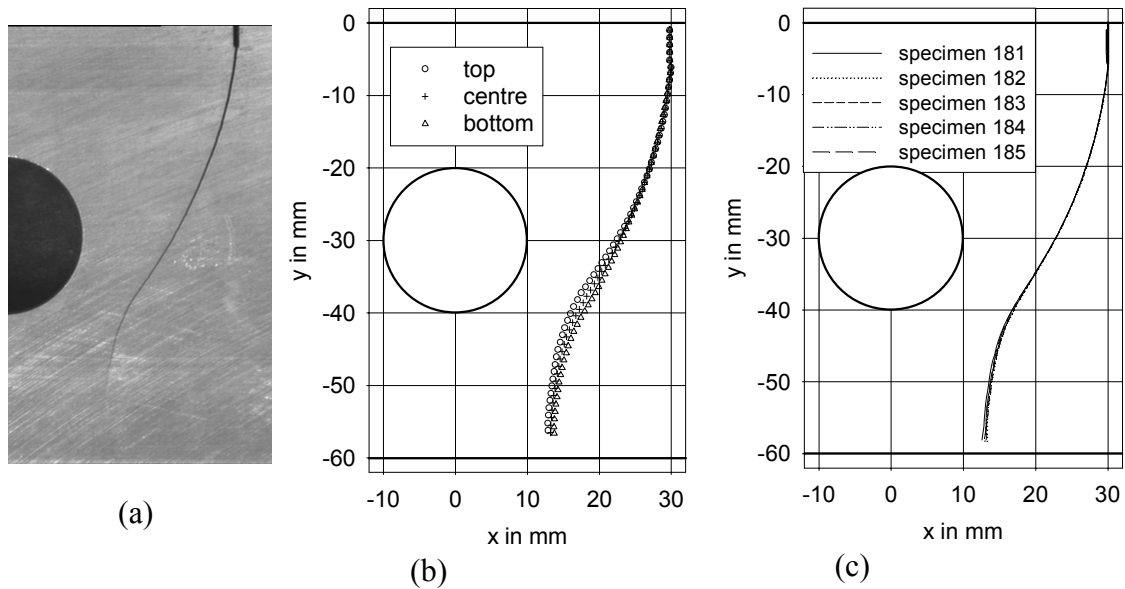


Figure 7. Experimental scattering of the fatigue crack paths of specimens  $a_N = 30$  mm  
 (a) crack path of specimen 185, (b) crack twisting of specimen 185, (c) crack paths at the centre line of all tested specimens with  $a_N = 30$  mm.

In Fig. 6 LFBH specimens are shown with experimentally obtained curved fatigue crack path for three of the eight tested notch positions. As an example the experimental findings of specimen 185 are given in Fig. 7. It can be recognised that the fatigue cracks are slightly twisted. But the crack path scattering at the centre line of all tested specimens of each notch position is very small.

## CRACK PATH SIMULATION

For the finite element calculations the models are chosen in accordance with the design of the LFBH specimen and the available test assembly, Fig. 8.

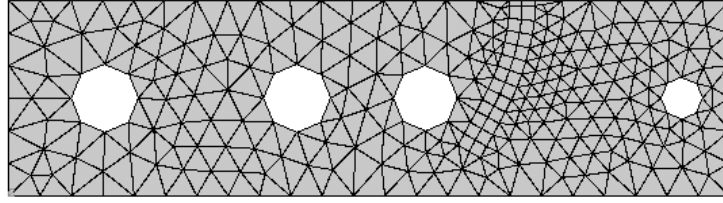


Figure 8. Finite element mesh of the specimen  $a_N = 30$  mm with steps  $\Delta h = 4$  mm.

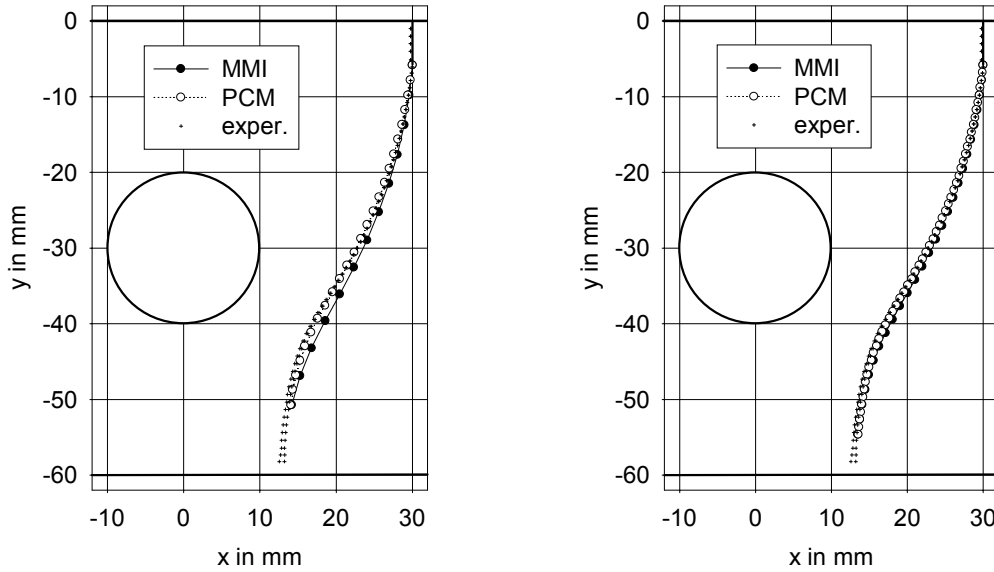


Figure 9. Simulated and experimentally obtained crack path specimen  $a_N = 30$  mm (a)  $\Delta h = 4$  mm; (b)  $\Delta h = 2$  mm. (curved incremental steps with marked mid-side nodes).

Table 1: Effect of the calculation method and the step width  $\Delta h$  on the mode I SIF

a/b	$K_I / \sigma_b \sqrt{\pi a}$					
	1.order MVCCI-method			Improved MVCCI-method		
	$\Delta h=1$ mm	$\Delta h=2$ mm	$\Delta h=4$ mm	$\Delta h=1$ mm	$\Delta h=2$ mm	$\Delta h=4$ mm
0,0970	0,62526	0,61953	0,61125	0,63035	0,63056	0,62988
0,2303	0,71541	0,71265	0,70484	0,71972	0,72141	0,72261
0,3637	0,90671	0,90407	0,89377	0,91216	0,91472	0,91565
0,4970	1,19753	1,19416	1,17843	1,20495	1,20799	1,20678
0,6303	1,58657	1,58249	1,56193	1,59600	1,59935	1,59934
0,7637	2,29515	2,27448	2,23815	2,31025	2,30614	2,29446
0,8970	5,23211	5,11896	4,86954	5,30440	5,27075	5,15710

All calculations were carried out fully automatically with a special implemented program in APDL of the FE-code ANSYS<sup>®</sup>. In Fig. 9 the numerical results for the incre-

ments  $\Delta h = 2\text{mm}$  and  $\Delta h = 4\text{mm}$  of the notch position  $a_N = 30\text{ mm}$  are given together with the scattering of the experimental findings. An excellent agreement is found also in cases with comparatively wide mesh divisions. Additional calculations were carried out without the proposed corrector step with straight increments (**mixed mode interpretation, MMI**) in order to verify the improved convergence of the proposed method. In particular for specimens with notch positions  $a_N = 30\text{ mm}$  the new method results in an accurate crack path. It was found that especially as the consequence of the MVCCI method in conjunction with the multiple mesh analysis ( $h_1/h_2 = 2$ ) the computed relation  $K_I(a)$  is very accurate also in the case of the step width  $\Delta h = 4\text{ mm}$ , Table 1.

## SUMMARY

This investigation has shown that the new predictor-corrector procedure in combination with the improved MVCCI method provides excellent crack path simulation results with 8-noded quadrilaterals and only moderately refined finite-element meshes around the crack tip. The step-by-step higher order simulation process with a piece by piece parabolic curved approximation of the crack path offers an excellent method for the numerical analysis of fatigue crack growth in complex two-dimensional structures. From the excellent agreement of the numerical and experimental results one can also conclude that the applied criterion of local symmetry provides a correct and reliable basis.

## REFERENCES

1. Bergkvist, H. and Gnex, L. (1978) *International Journal of Fracture* **5**, 429-441.
2. Sumi, Y. (1985) *Theoretical and Applied Fracture Mechanics* **4**, 149-156.
3. Sumi, Y. (1990) *International Journal of Fracture* **44**, 189-207.
4. Portela, A. and Aliabadi, M.H. (1992) *Crack Growth Analysis Using Boundary Elements*. Computational Mechanics Publication Publisher, Southampton, UK.
5. Theilig, H., Döring, R. and Buchholz, F.-G. (1997) In: *Advances in Fracture Research, ICF9*, Volume 4, pp. 2235-2242, B. L. Karahaloo, Y.-W. Mai, M. I. Ripley, R. O. Ritchie, (Eds.). Pergamon, Amsterdam-Oxford-New York-Tokyo-Lausanne.
6. Theilig, H. and Buchholz, F.-G. (2001) In: *Advances in Fracture Research, ICF10*, K. Ravi-chandar, B.L. Karahaloo, T. Kishi, R.o.Ritchie, A.T.Yokobori Jr, T.Yokobori, (Eds) Published by Elsevier Science Ltd, Oxford, UK.
7. Theilig, H. and Buchholz, F.-G. (2001) In: *Proceed. of the 6<sup>th</sup> Int. Conf. On Biaxial / Multiaxial Fatigue and Fracture*, Vol. II, pp. 631-638, M. Moreira de Freitas(Ed.), Edt. by Instituto Superior Technico, Lisboa.
8. Buchholz, F.-G. (1984) In: *Accuracy, Reliability and Training in FEM-Technology*, pp. 650-659, Robinson, I. (Ed.). Robinson and Associates, Dorset.
9. Theilig, H. (1981) *Maschinenbautechnik* **30**, 79-83.
10. Theilig, H. (1982) *Kernenergie* **25**, 173-176.
11. Theilig, H. (1984) *Technische Mechanik* **5**, 31-36.